An Intensity Index for the East Asian Winter Monsoon

LIN WANG AND WEN CHEN

Center for Monsoon System Research, Institute of Atmospheric Physics, Chinese Academy of Sciences, Beijing, China

(Manuscript received 7 February 2013, in final form 15 October 2013)

ABSTRACT

The thermal contrast between the Asian continent and the adjacent oceans is the primary aspect of the East Asian winter monsoon (EAWM) that can be well represented in the sea level pressure (SLP) field. Based on this consideration, a new SLP-based index measuring the intensity of the EAWM is proposed by explicitly taking into account both the east–west and the north–south pressure gradients around East Asia. The new index can delineate the EAWM-related circulation anomalies well, including the deepened (shallow) midtropospheric East Asian trough, sharpened and accelerated (widened and decelerated) upper-tropospheric East Asian jet stream, and enhanced (weakened) lower-tropospheric northerly winds in strong (weak) EAWM winters. Compared with previous indices, the new index has a very good performance describing the winter-mean surface air temperature variations over East Asia, especially for the extreme warm or cold winters. The index is strongly correlated with several atmospheric teleconnections including the Arctic Oscillation, the Eurasian pattern, and the North Pacific Oscillation/western Pacific pattern, implying the possible internal dynamics of the EAWM variability. Meanwhile, the index is significantly linked to El Niño–Southern Oscillation (ENSO) and the sea surface temperature (SST) over the tropical Indian Ocean. Moreover, the SST anomalies over the tropical Indian Ocean are more closely related to the index than ENSO as an independent predictor. This adds further knowledge to the prediction potentials of the EAWM apart from ENSO. The predictability of the index is high in the hindcasts of the Centre National de Recherches Météorologiques (CNRM) model from Development of a European Multimodel Ensemble System for Seasonal-to-Interannual Prediction (DEMETER). Hence, it would be a good choice to use this index for the monitoring, prediction, and research of the EAWM.

1. Introduction

A simple and representative index is useful in East Asian winter monsoon (EAWM) studies. It could help to delineate the variability and to understand the mechanism of the EAWM. Besides, it could benefit the monitoring and prediction of the EAWM in operational climate centers. Wang and Chen (2010) reviewed and compared the performances of 18 EAWM indices. They classified these indices into four categories: low-level wind indices (e.g., Chen et al. 2000), upper zonal wind shear indices (e.g., Jhun and Lee 2004), east–west pressure contrast indices (e.g., Wu and Wang 2002), and East Asian trough indices (e.g., Sun and Li 1997). These four groups of indices reflect, to some extent, the current understanding of the EAWM variability.

The use of sea level pressure (SLP) has several advantages in defining the EAWM index. On one hand, the EAWM is primitively driven by the thermal contrast between the cold Asian continent and adjacent warm oceans (e.g., Trenberth et al. 2006). This nature could be well indicated in the SLP field, in which the Siberian high is surrounded by the Aleutian low to its east and a low pressure center around the Maritime Continent (hereafter referred as the MC low) to its south (Fig. 1a). To our knowledge, the earliest EAWM index was defined with SLP (Xu and Ji 1965). On the other hand, compared with near-surface wind and other upper- and midtropospheric meteorological variables, both the availability and the quality of the SLP data are good, especially in the period before the 1940s. Hence, SLP-based indices are more reliable and convenient to investigate the historical variations of the EAWM.

It is generally believed that the east–west pressure gradient between the Siberian high and the Aleutian low is dominant for the formation and variability of the EAWM. The existing SLP-based indices were mainly

Corresponding author address: Dr. Lin Wang, Institute of Atmospheric Physics, Chinese Academy of Sciences, P.O. Box 2718, Beijing 100190, China.
E-mail: wanglin@mail.iap.ac.cn

DOI: 10.1175/JCLI-D-13-00086.1

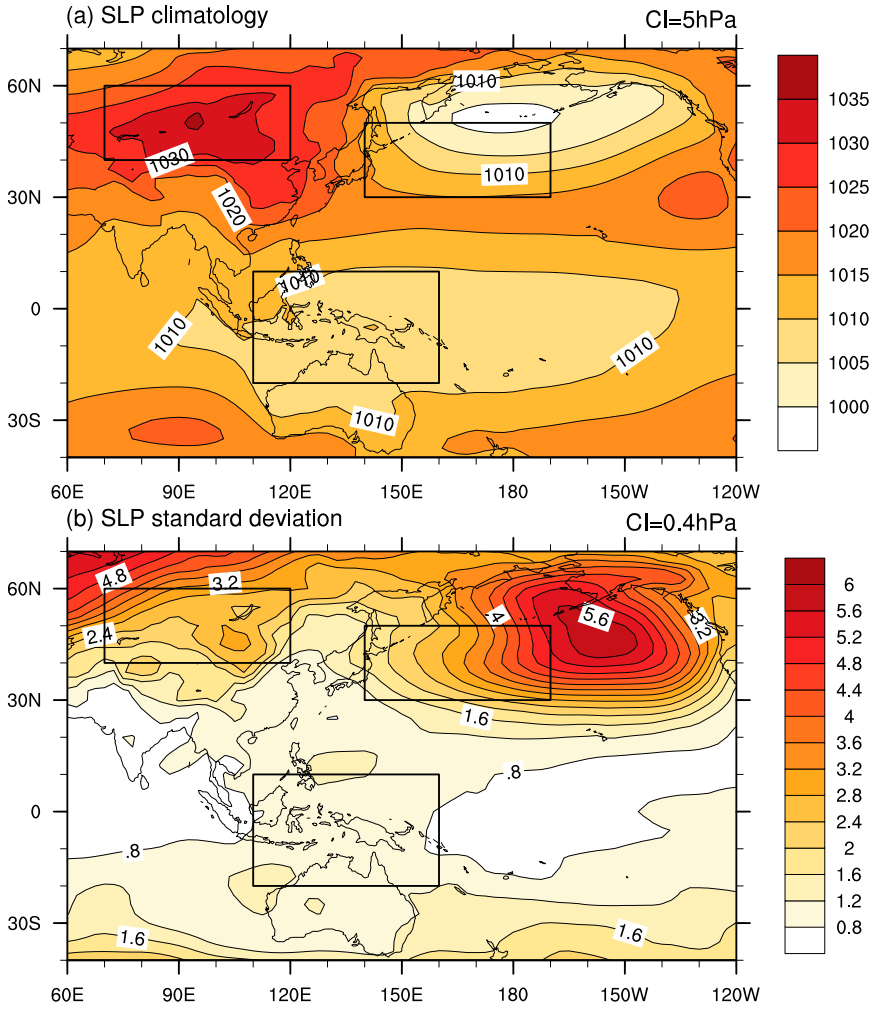

FIG. 1. (a) The climatology of winter [December–February (DJF)]-mean SLP averaged for the period 1957–2001. (b) The distribution of the std dev of SLP in boreal winter for the period 1957–2001. Contour intervals (CI) are 5 hPa in (a) and 0.4 hPa in (b). The three rectangles indicate the areas used to define the EAWM index.

defined to reflect this feature [e.g., Xu and Ji 1965; Wu and Wang 2002; see Wang and Chen (2010) for a review]. However, it is noteworthy that the north–south pressure contrast between the Siberian high and the MC low is also important for the EAWM. In the climatological mean sense, the near-surface winds associated with the EAWM are generally northwesterly to the north of about 30°N and northeasterly to the south of this latitude (e.g., Chen et al. 2000; Chang et al. 2006). The formation of this northeasterly is partly due to the shape of the East Asian coasts and partly related to the pressure gradient between the Siberian high and the MC low. On intraseasonal and interannual time scales, the variations of the EAWM are related to intense tropical–extratropical interactions (Chang et al. 2006, 2011). When the EAWM is anomalously strong, above-normal SLP is usually observed in the midlatitudes because of the amplification of the Siberian high (e.g., Zhang et al. 1997; Takaya and Nakamura 2005). Meanwhile, below-normal SLP could be observed around the Maritime Continent due to the enhanced cold surge activities and resultant increased convection and precipitation there (e.g., Chang et al. 2006; Wang and Chen 2010). This out-of-phase variation of SLP between the Siberian high and the MC low increases the north–south pressure gradient. These facts suggest that the north–south pressure gradient is a basic and important feature associated with the EAWM variations, which is as important as the east–west pressure gradient (section 7a), and should be taken into account when the EAWM index is defined (Liu 2007). However, this feature was not reflected explicitly in previous SLP-based EAWM indices (Wang and Chen 2010).

In this study, we propose an SLP-based index to measure the intensity of the EAWM by taking both the east–west and the north–south pressure contrasts into account. Section 2 describes the datasets and section 3 defines the new EAWM index. Section 4 then delineates the circulation, temperature, and precipitation anomalies represented by the new index. The associations with sea surface temperature (SST) and potential predictability of the index are elucidated in section 5. Finally, a summary and discussion are provided in sections 6 and 7, respectively.

2. Data

The atmospheric variables used in this study are from the monthly mean 40-yr European Centre for Medium-Range Weather Forecasts (ECMWF) Re-Analysis (ERA-40) dataset, which covers 45 years from September 1957 to August 2002 (Uppala et al. 2005). This dataset has a 2.5° × 2.5° horizontal resolution and extends from 1000 to 1 hPa with 23 vertical pressure levels. The oceanic data are the Hadley Centre Sea Ice and Sea Surface Temperature dataset, version 1 (HadISST1; Rayner et al. 2003), which has a 1° × 1° resolution and spans from 1870 to the present. The monthly global Precipitation Reconstruction dataset (PREC) that covers both land and ocean is from the National Oceanic and Atmospheric Administration (NOAA) Climate Prediction Center (CPC) (Chen et al. 2002). The land portion of this data is defined by optimum interpolation of gauge observations at over 17 000 stations in the world. The oceanic part is produced by an empirical orthogonal function (EOF) reconstruction of historical gauge observations over islands and land areas (Chen et al. 2003). The PREC has a 2.5° × 2.5° resolution and is updated for an extended period longer than 50 years from 1948 to the present. We also use the monthly-mean surface air temperature and precipitation from 160 Chinese stations provided by the China Meteorological Administration. This dataset starts from 1951 and updates every month to the present.

In addition to the reanalysis and observational data, the hindcasts from Development of a European Multimodel Ensemble System for Seasonal-to-Interannual Prediction (DEMETER) coupled general circulation models (CGCMs) (Palmer et al. 2004) are also employed to examine the predictability of the new index. Three out of seven CGCMs (SCWF from ECMWF, CNRM from Météo-France, and UKMO from the Met Office) are selected because they span periods almost identical to that of the ERA-40 dataset. The hindcasts starting from November are employed so that the data of the whole winter are available. All nine separate runs with different initial conditions are used for each model. The period analyzed in this study is from September 1957 to August 2002. Seasonal means are considered and they are constructed from the monthly means by averaging the data of DJF, which results in 45 winters (1957–2001). Here, the winter of 1957 refers to the 1957/58 winter.

3. Definition of the EAWM index

Figure 1a shows the climatology of the winter-mean SLP field. The pressure systems including the Siberian high, the Aleutian low, and the MC low are easy to recognize. On the interannual time scale, the variability of the MC low is large over the Maritime Continent as revealed by the standard deviation of SLP (Fig. 1b), roughly coinciding with the climatological center of the MC low. This large variability, which is the largest in the tropical region (not shown), could be partly accounted for by the intense tropical–extratropical interactions associated with the EAWM involving cold surge–induced enhanced tropical convective activity and the resultant wave train–like teleconnections emanating from the tropics toward the midlatitudes (e.g., Lau et al. 1983; Neale and Slingo 2003). The Siberian high's variability center also roughly overlaps with its climatological center although the variability of SLP is much larger to the northwest of the central Siberian high (Fig. 1b). Regarding the Aleutian low, in contrast, the center of variability is located to the east of its climatological center (Fig. 1b), possibly due to the influence of El Niño–Southern Oscillation (ENSO) via a Pacific–North American (PNA)-like Rossby wave train (e.g., Trenberth et al. 1998). This variability center extends westward to the south of about 50°N, indicating large variance over the southwestern portion of the Aleutian low. In fact, previous studies indicated that the SLP in the southwestern portion of the Aleutian low is more significantly related to the EAWM than that in the center of the Aleutian low [e.g., Fig. 9a of Wu et al. (2006) and Figs. 4a–9a of Wang and Chen (2010)].

Based upon the above analysis and taking into account both the east–west and the north–south pressure gradients, an EAWM index is proposed as below:

$$I_{\mathrm{EAWM}} = (2 \times \mathrm{SLP}_1^* - \mathrm{SLP}_2^* - \mathrm{SLP}_3^*)/2,$$

where SLP_1^*, SLP_2^*, and SLP_3^* indicate the normalized area-averaged SLP over Siberia (40°–60°N, 70°–120°E), the North Pacific (30°–50°N, 140°E–170°W), and the Maritime Continent (20°S–10°N, 110°–160°E), respectively. Here, the normalized instead of the raw SLP is used because the variance of SLP is small in the tropical region compared with that in the midlatitudes (Fig. 1b). Such a procedure could increase the weighting of tropical

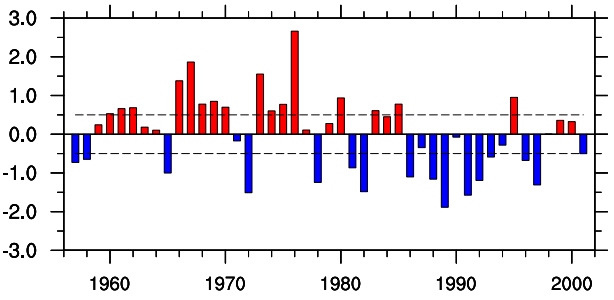

FIG. 2. Normalized DJF-mean EAWM index for the period 1957–2001. Two dashed lines indicate ±0.5 std dev.

SLP in the index. Nevertheless, the employment of the normalized SLP does not lead to an obvious overestimation of the role of the tropics in the variability of the EAWM. As will be discussed in sections 7b and 7c, the correlation coefficient is 0.99 between the indices using the normalized and the raw SLP for the 45 years concerned. Moreover, the index based on the normalized SLP has better predictability than that based on the raw SLP in DEMETER CGCMs.

Figure 2 shows the normalized EAWM index for the period 1957–2001, where the positive index indicates strong EAWM. It features clear interannual variations and captures the decadal weakening of the EAWM around the mid-1980s well (e.g., Nakamura et al. 2002; Jhun and Lee 2004; Wang et al. 2009b). In the following section, a composite analysis is performed to reveal the climate anomalies associated with this index. The 0.5 standard deviation is used to select strong and weak EAWM cases. Based on this criterion, 16 (16) winters are identified as strong (weak) EAWM years (Table 1).

4. Climate anomalies represented by the EAWM index

a. Circulation

Figure 3 shows the composite circulation differences between strong and weak EAWM winters. Significant positive SLP anomalies over the Eurasian continent indicate an intensified Siberian high (Fig. 3a). Although the center of SLP anomalies is located around the Ural Mountains (Fig. 3a) due to the large variability in that region (Fig. 1b), the correlation coefficient between the EAWM index and the Siberian high index (Gong et al. 2001) is 0.89 for the period 1957–2001, far beyond the 99.9% confidence level. This is consistent with previous studies that the Siberian high is a key system for the EAWM (e.g., Gong et al. 2001; Takaya and Nakamura 2005; Chang et al. 2011). Over the North Pacific area, the SLP anomalies are negative to the southwest of the Aleutian Islands and positive around the Bering Sea, resembling the negative phase of the North Pacific Oscillation (NPO; Wallace and Gutzler 1981; Linkin and Nigam 2008). The negative SLP anomalies extend southwestward to the Maritime Continent and farther westward to the tropical Indian Ocean, Africa, and the tropical Atlantic Ocean with a high confidence level. These results indicate that the new index not only reflects the enhanced east–west pressure contrast associated with the strong EAWM, consistent with previous EAWM indices (e.g., Wang and Chen 2010), but also captures the enhanced north–south pressure contrast associated with the strong EAWM that was not well delineated in most of the previous EAWM indices. Note that the SLP anomalies are most significant over the Eurasian continent and the adjacent ocean to its east and south, whereas those in other regions (e.g., the tropical eastern Pacific) are less significant. It further suggests that the new EAWM index is good at describing the thermal contrast between cold Asian continent and adjacent warm oceans, which is the nature of the EAWM.

In the midtroposphere, a remarkable feature is the negative geopotential height anomalies spanning the whole tropical region (Fig. 3b). It coincides with the SLP field (Fig. 3a) and implies a close connection between the EAWM and the tropics. In the extratropical Northern Hemisphere, the negative geopotential height anomalies around Japan indicate a deepened East Asian trough in strong EAWM winters. The accompanied feature is a wave train–like anomaly stretching from Europe to East Asia and a dipole-like anomaly over northeast Asia. The two patterns quite resemble the Eurasian (EU) and the western Pacific (WP) teleconnections (Wallace and Gutzler 1981). This is consistent with the composite of the SLP field, which exhibits clear NPO-like anomalies (Fig. 3a)—the surface signature of the WP pattern (Linkin and Nigam 2008). The correlation coefficient between the EAWM index and the EU (NPO/WP) index is 0.77 (−0.57/−0.63), far beyond the 99.9% confidence level (Table 2). These coefficients are higher than that with the Arctic Oscillation (AO; Thompson and Wallace 1998) (−0.47; Table 2), implying that the EU and NPO/WP

TABLE 1. Strong and weak EAWM winters selected for composite. Superscripts *E* and *L* denote El Niño and La Niña events according to the definition of CPC/NOAA.

Strong	1960, 1961, 1962, 1966, 1967, 1968^{E}, 1969^{E}, 1970^{L}, 1973^{L}, 1974^{L}, 1975^{L}, 1976^{E}, 1980, 1983^{L}, 1985, 1995^{L}
Weak	1957^{E}, 1958^{E}, 1965^{E}, 1972^{E}, 1978, 1981, 1982^{E}, 1986^{E}, 1988^{L}, 1989, 1991^{E}, 1992, 1993, 1996, 1997^{E}, 2001

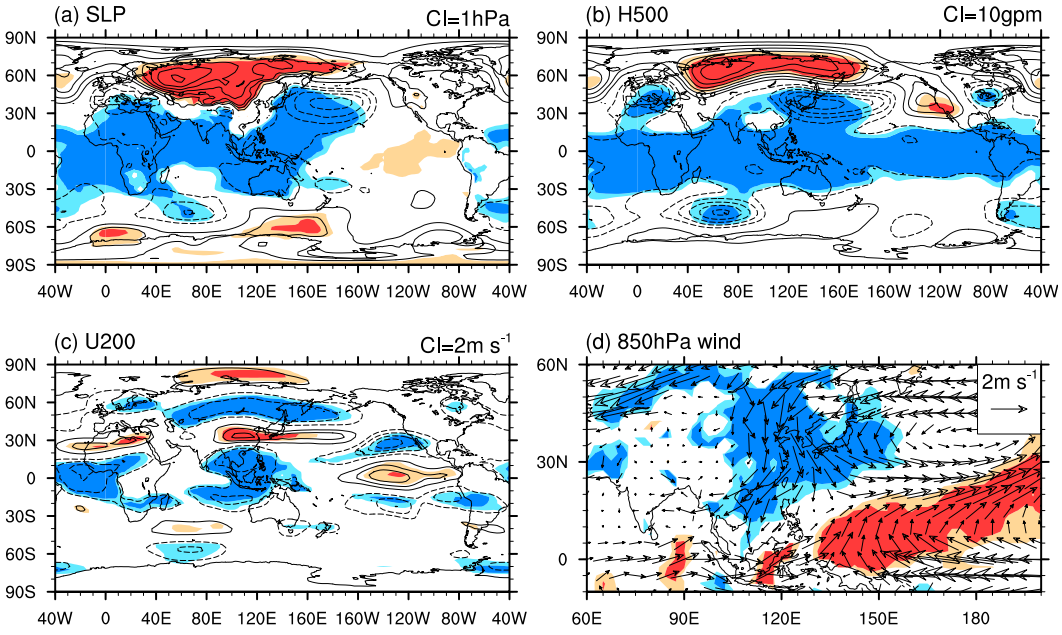

FIG. 3. Composite differences of DJF-mean (a) SLP, (b) 500-hPa geopotential height, (c) 200-hPa zonal winds, and (d) 850-hPa wind vector ($m\,s^{-1}$) between strong and weak EAWM winters. CI are 1 hPa in (a), 10 gpm in (b), and $2\,m\,s^{-1}$ in (c). Zero contours are omitted and negative values are dashed. Light and dark shading indicate the 95% and 99% confidence levels based on a two-sided Student's *t* test, respectively.

patterns are likely to be more closely related to the EAWM variations than the AO on the interannual time scale.

In the upper troposphere, the strong EAWM represented by the new index is featured with a sharpened and accelerated East Asian jet stream (Fig. 3c), consistent with previous indices (e.g., Jhun and Lee 2004; Li and Yang 2010). The zonal wind anomalies over the tropical and subtropical eastern Pacific are similar to those related to ENSO (e.g., Yang et al. 2002). In the lower troposphere, significant northerly wind anomalies are observed from Lake Baikal to the South China Sea in the meridional direction and from eastern China to the east of Japan in the longitudinal direction (Fig. 3d). This suggests that the enhanced northerly wind over East Asia in strong EAWM cases can be well delineated by the new index.

b. Temperature and precipitation

Figure 4 shows the composite map of precipitation and temperature anomalies in strong EAWM winters. Accompanied with the well-delineated EAWM-related circulation anomalies, enhanced precipitation is observed over the Maritime Continent, while reduced precipitation is observed over the midlatitude continent and along the EAWM front extending from southeast China across the south of Japan to the northwest Pacific (Fig. 4a). This is in agreement with previous studies showing that strong EAWM facilitates enhanced precipitation in low latitudes and suppressed precipitation over midlatitudes (e.g., Sun and Li 1997; Wang and Chen 2010; Wang and Feng 2011). This feature is confirmed with the station observations, which show reduced precipitation in southeast China (Fig. 4c).

In strong EAWM winters, significant cooling is observed from central Siberia to temperate East Asia, and farther southward to the South China Sea, the Maritime Continent, and the Indian Ocean (Fig. 4b). The correlation coefficients between the EAWM index and the two temperature modes over East Asia (B. Wang et al.

TABLE 2. Simultaneous correlation coefficients *r* between the EAWM index and selected climatic indices for the period 1957–2001. One and two asterisks (* and **) indicate that the correlation coefficients exceed the 99% and 99.9% confidence levels based on a two-sided Student's *t* test, respectively.

Index	*r*	Reference
SH	0.89**	Gong et al. (2001)
EU	0.77**	Wallace and Gutzler (1981)
WP	−0.63**	CPC/NOAA
NPO	−0.57**	Linkin and Nigam (2008)
AO	−0.47*	Thompson and Wallace (1998)
T_{north}	0.44*	B. Wang et al. (2010), northern mode
T_{south}	0.67**	B. Wang et al. (2010), southern mode
Niño-3	−0.49**	SST (5°S–5°N, 150°–90°W)
TIO	−0.58**	SST (10°S–10°N, 40°–90°E)

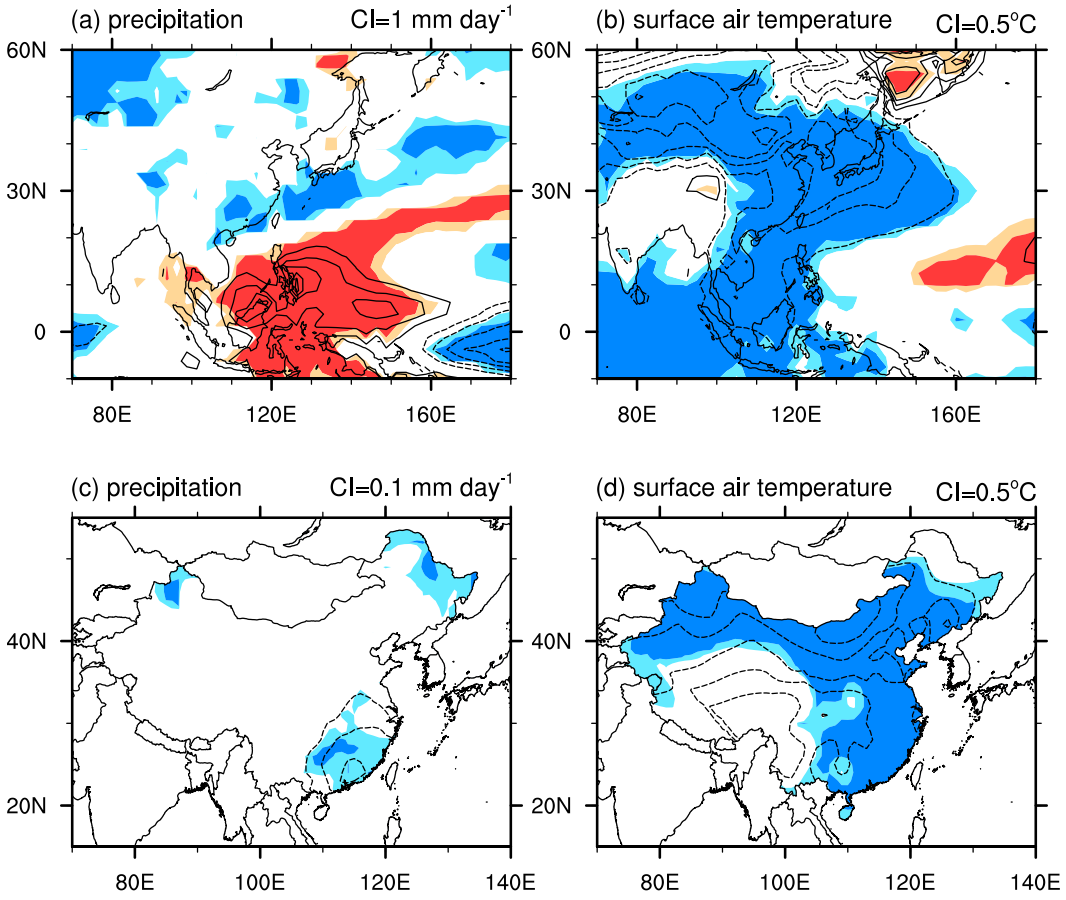

FIG. 4. Composite differences of DJF-mean (a) precipitation based on PREC and (b) surface air temperature based on ERA-40 between strong and weak EAWM winters. (c),(d) As in (a),(b), but based on observations from 160 China stations. CI are 1 mm day^{-1} in (a), 0.1 mm day^{-1} in (c), and 0.5°C in (b) and (d). Zero contours are omitted and negative values are dashed. Light and dark shading indicate the 95% and 99% confidence levels based on a two-sided Student's t test, respectively.

2010) are calculated. The new index is more closely linked to the southern mode (T_{south}) than the northern mode (T_{north}) of East Asian temperatures (Table 2). We specifically look at the surface air temperature anomalies in China. Cooling with a high confidence level is observed in large areas of mainland China except the Tibetan Plateau and marginal areas of northeast China (Fig. 4d). It indicates that despite the complex topography, this index has good performance in describing the temperature variations over East Asia, especially over China. In this aspect, the performance of the new index is better than all the indices illustrated in Wang and Chen (2010).

To further reveal the performance of the new index, a comparison was made between the new index and all EAWM indices listed in Wang and Chen (2010) as well as two more indices (Zhu 2008; Li and Yang 2010). The scatterplots in Fig. 5 present the covariability of the EAWM indices with the winter-mean surface air temperature anomalies averaged over East Asia (20°–50°N, 100°–145°E; Boo et al. 2011) based on ERA-40. Among the 20 indices that take part in the comparison, the correlation coefficient between the new index and the East Asian surface air temperature ranks number 2 ($r = -0.77$; Fig. 5a), which is only slightly lower than that of the Cui and Sun (1999) index ($r = -0.78$; Fig. 5r). In contrast, the new index has better performance than Cui and Sun (1999) to delineate the extreme phase of the EAWM (i.e., extreme warm/cold winters). Taking a 0.5 standard deviation and ±0.5°C as a criterion for the EAWM indices and the temperature anomalies, respectively, the relationship between the strength of the EAWM and the surface air temperature extremes over East Asia is best represented by the new index (Fig. 5). For the 45-yr period concerned, the high (low) EAWM index corresponds to 10 (10) extreme cold (warm) winters over East Asia. This performance is the best among all the 20 indices (Fig. 5). The same conclusion can be drawn when the surface air temperature over China is

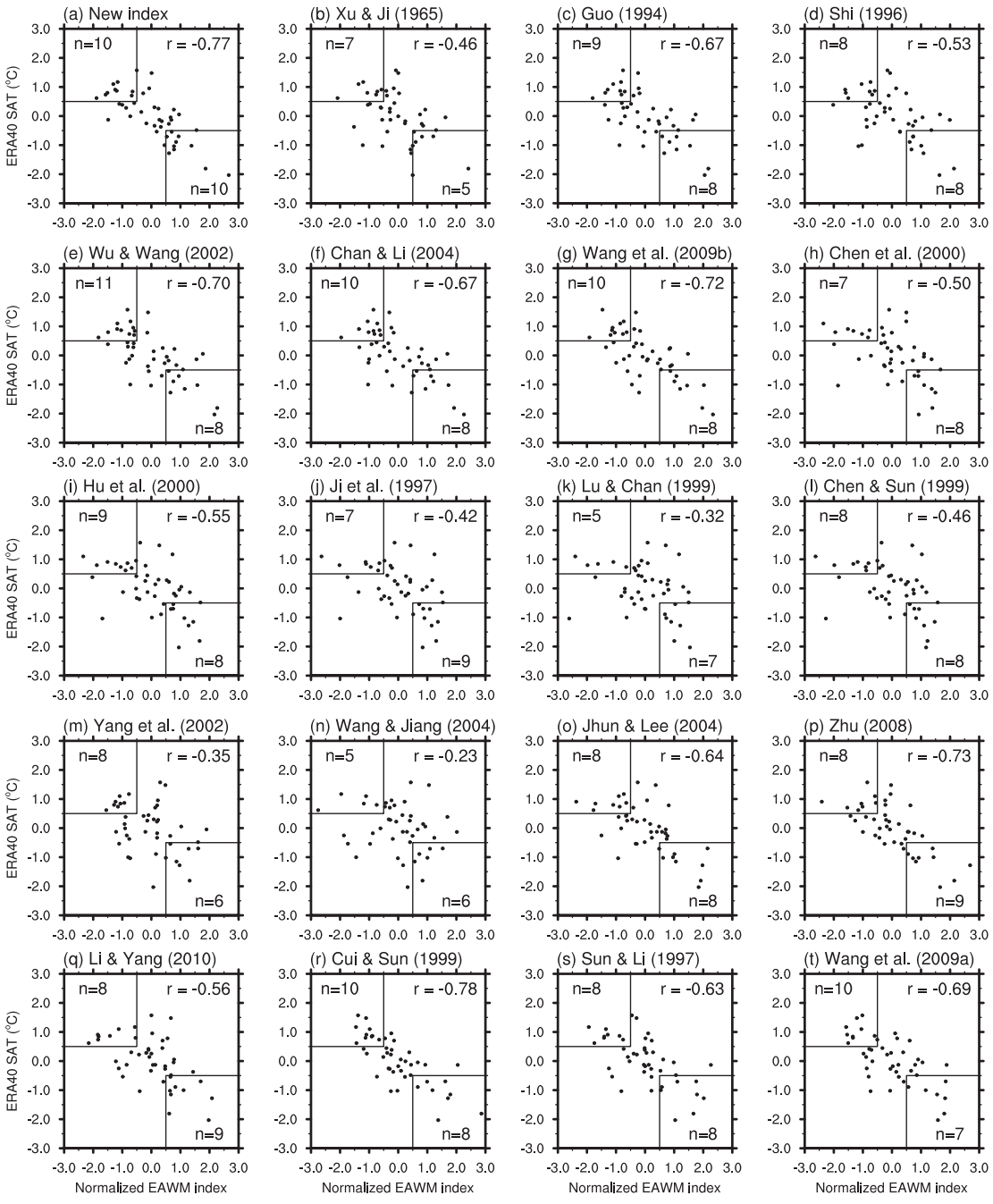

FIG. 5. Scatterplots of normalized EAWM index vs DJF-mean surface air temperature anomalies averaged over East Asia (20°–50°N, 100°–145°E; ERA-40) for the period 1957–2001 based on the EAWM index defined in (a) this paper and (b)–(t) 19 other papers listed in the references. The abscissa (ordinate) of each dot in each diagram represents the amplitude and sign of the EAWM index (the temperature index) for an individual winter season. The number of the low (high) EAWM index with warm (cold) winter is shown at the upper left (lower right) corner of each plot. The correlation coefficient between the EAWM index and temperature index is shown in the upper right corner of each plot.

concerned based on the 160 Chinese station data values (Fig. 6). The new index ranks number 2 in the aspect of the correlation coefficient (Figs. 6a,r) and ranks jointly as number 1 in the aspect of representing extreme temperature conditions in China (Figs. 6a,e). These results suggest that the new index has very good performance to delineate the variations of the EAWM, especially for extreme cold/warm winters.

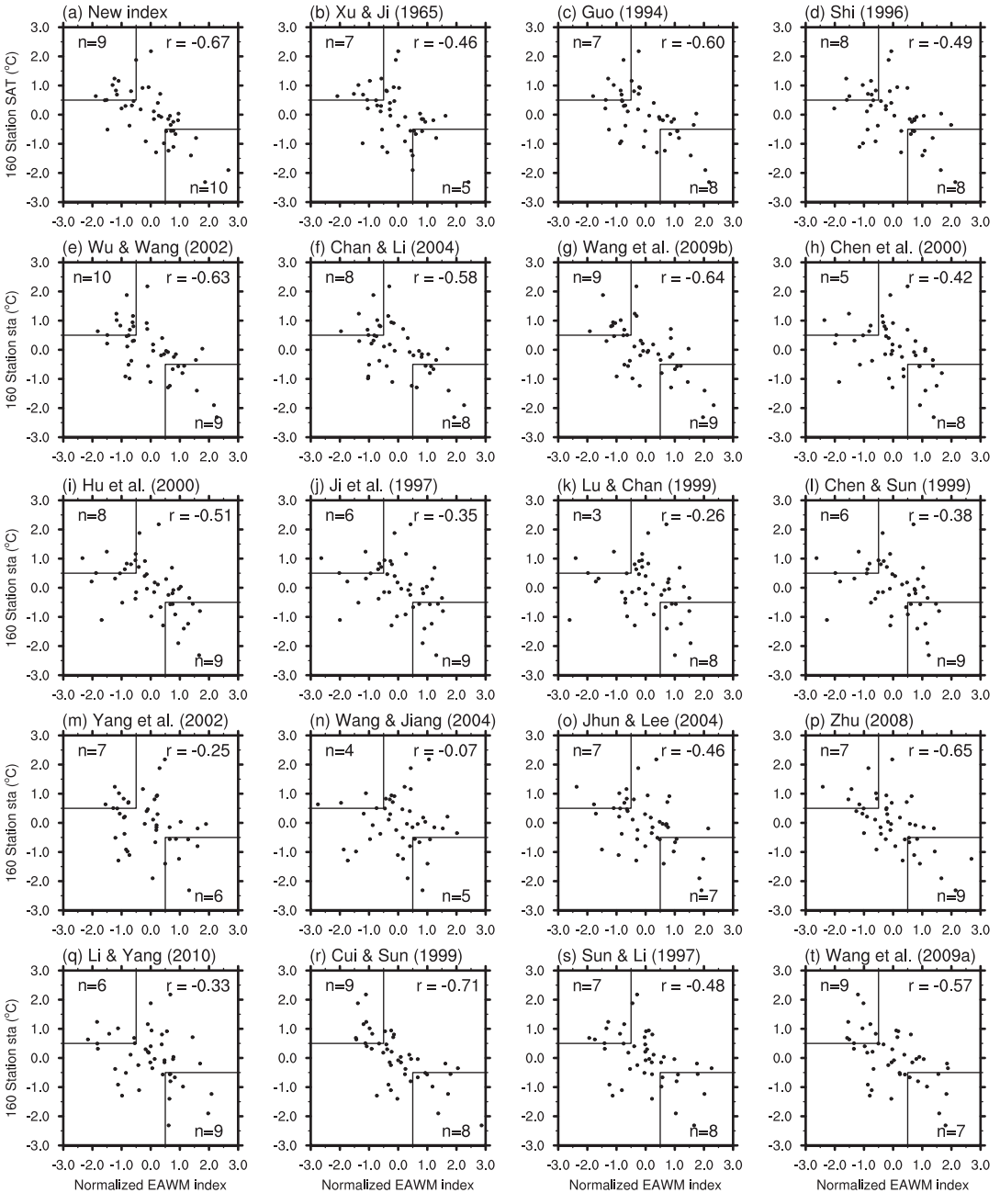

FIG. 6. As in Fig. 5, but for the DJF-mean surface air temperature anomalies averaged over China with 160 Chinese stations.

5. Predictability of the EAWM revealed by the new index

a. In observations

The ocean is an important origin of the predictability of the EAWM on the interannual time scale, so we investigated the associations of the new EAWM index with SST. Table 1 indicates that according to the definition of ENSO in CPC/NOAA, 6 (3) out of 16 strong EAWM cases are La Niña (El Niño) winters and 8 (1) out of 16 weak EAWM cases are El Niño (La Niña) winters. This implies that strong (weak) EAWM cases are more likely to be observed when La Niña (El Niño) occurs, consistent with previous studies (e.g., Zhang et al. 1997; Chen et al. 2000, 2006). Figure 7 exhibits the composite difference of SST anomalies between strong and weak EAWM

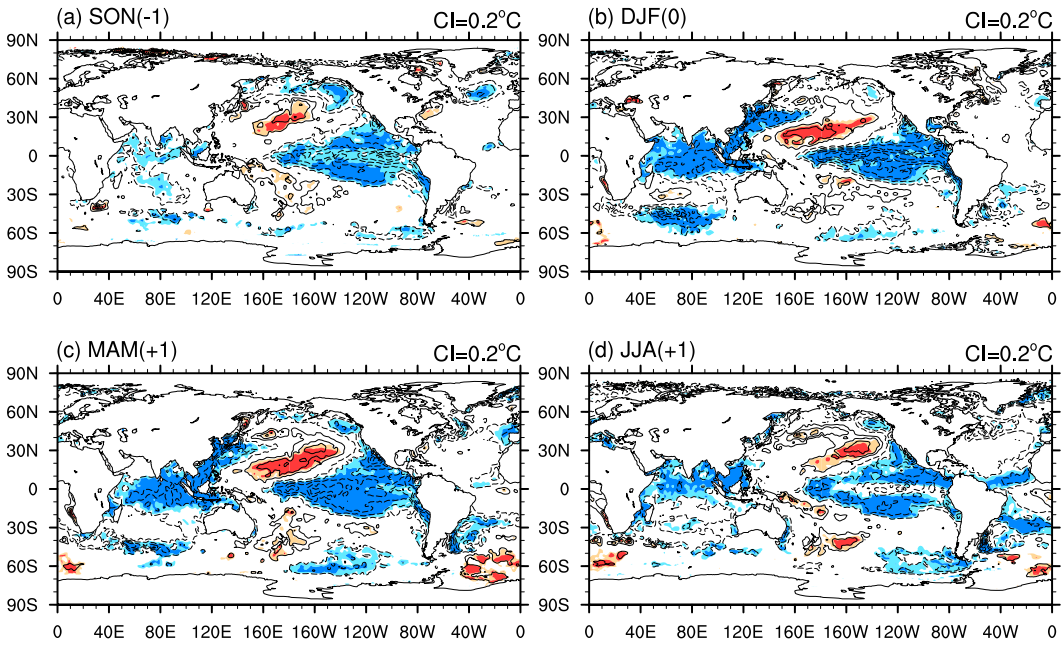

FIG. 7. Composite SST anomalies in (a) the preceding autumn [September–November (SON)], (b) the simultaneous DJF, (c) the following spring [March–May (MAM)], and (d) the following summer [June–August (JJA)] between strong and weak EAWM years. CI are 0.2°C. Zero contours are omitted and negative values are dashed. Light and dark shading indicate the 95% and 99% confidence levels based on a two-sided Student's *t* test, respectively.

years. The dominant feature in the simultaneous winter is the negative SST anomalies in the tropical eastern Pacific, in the tropical Indian Ocean (TIO) and along the coasts of East Asia (Fig. 7b), resembling the typical mature phase of La Niña. The lead/lag composite indicates that the SST anomalies in both the tropical eastern Pacific and the TIO can be traced back to the preceding autumn (Fig. 7a) and persist to the following spring and summer (Figs. 7c,d). This feature can further be seen from the lag correlations between the EAWM index and the average SST anomalies over the Niño-3 region (5°S–5°N, 150°–90°W; Fig. 8a) and the TIO (10°S–10°N, 40°–90°E; Fig. 8b). Although clear warming trends are observed in the Indian Ocean in recent decades (Alory et al. 2007), the above results remain almost the same if the linear trends are removed (not shown). Hence, it suggests that the SST anomalies in these regions are likely to act as driving factors for the EAWM.

The influences of ENSO on the EAWM have been widely accepted, so the possible argument here is whether the impact of the Indian Ocean on the EAWM is dependent on ENSO. In fact, previous studies have demonstrated that the Indian Ocean can exert influences that are independent of ENSO on the convection over the tropical western Pacific in boreal winter (e.g., Watanabe and Jin 2002; Annamalai et al. 2005). Besides, the ENSO-induced SST anomalies usually appear in the Indian Ocean approximately 3–6 months after the peak of ENSO (e.g., Lau and Nath 1996). In our composite, however, the negative SST anomalies begin to appear in autumn when the ENSO is still in its developing phase (Fig. 7a). Therefore, the SST anomalies in the TIO are not responses to ENSO, and can be identified as an independent potential predictor for the EAWM.

Note that the significant correlation (above the 95% confidence level) with the Niño-3 index leads peak winter by five months, while that with the TIO index leads peak winter by only three months (Fig. 8). In contrast, the amplitude of correlation coefficient is larger with the TIO index (−0.58) than with the Niño-3 index (−0.49) for simultaneous winter (Table 2, Fig. 8) and for a leading time of one month (Fig. 8). These results suggest that the prediction of the EAWM based on ENSO has a better leading time than that based on TIO SST, but the near-term prediction of the EAWM based on TIO SST may have a better performance, especially when the prediction is made in late autumn.

In addition to the SST, the Arctic sea ice of the preceding autumn is also closely linked to the variations of the EAWM, with below-normal autumn Arctic sea ice facilitating a strong EAWM (e.g., Wu et al. 1999; Honda et al. 2009; Wu et al. 2011). We examined this relationship with the new index. On the interannual time scale, the correlation coefficient between the September area-averaged Arctic sea ice concentration (SIC) over the

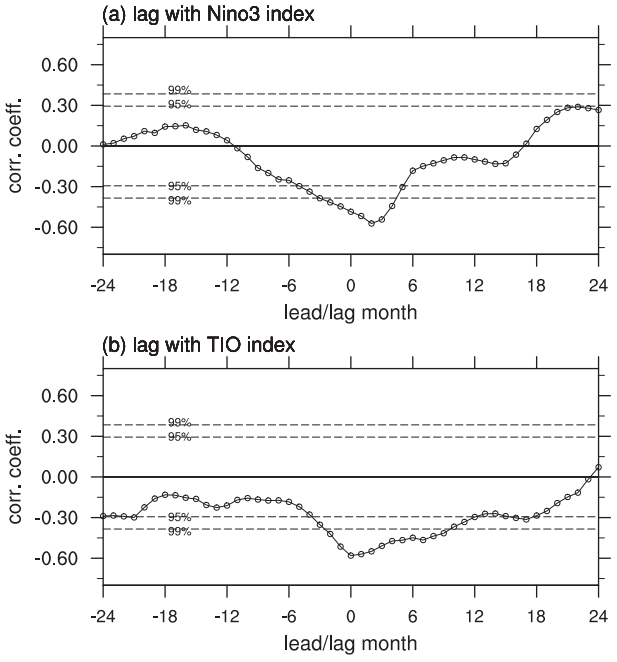

FIG. 8. Lag correlations between the EAWM index and SST anomalies averaged over (a) the tropical eastern Pacific (5°S–5°N, 150°–90°W) and (b) the tropical Indian Ocean (10°S–10°N, 40°–90°E). The data are smoothed by 3-month running means.

Kara–Laptev Seas (76.5°–83.5°N, 60.5°–149.5°E; Wu et al. 2011) and the EAWM index is −0.47 for the period 1979–2001, exceeding the 98% confidence level. On the decadal time scale, the recent amplification of the EAWM since the 2004 winter is accompanied with significant diminished Arctic SIC (Wang and Chen 2014). Hence, the potential influences of the Arctic sea ice could also be captured by the new index on both interannual and decadal time scales.

b. In DEMETER CGCMs

Finally, we assess the predictability of the new EAWM index in DEMETER CGCMs that have proved to have some skills in simulating the EAWM variations (e.g., Li and Wang 2012). Table 3 shows the prediction of the DJF-mean EAWM index in the nine-run ensemble with a lead time of one month (i.e., the prediction started from November). The EAWM index was best predicted in CNRM at the 99.9% confidence level but was poorly predicted in UKMO and SCWF. An inspection of individual runs indicates that 6 (2) out of 9 runs of CNRM can predict the EAWM index at the 98% (90%) confidence level, whereas only 2 (1) out of 9 runs of UKMO (SCWF) can predict the EAWM index at the 99% (90%) confidence level. This is consistent with previous analysis that CNRM has better performance in reproducing the EAWM variability than UKMO and SCWF (Li and Wang 2012). Because of the availability of the DEMETER model data (especially the SST data), it is difficult to identify the causes of the successful and unsuccessful prediction. Anyway, a substitutive analysis on the 2-m air temperature indicates that SCWF is not likely to be able to reproduce the relationship between the EAWM and SST of the tropical oceans (not shown), which might explain its worst performance among the three models (Table 3). In contrast, such a relationship is likely to be caught by UKMO (not shown). This might explain why 2 of the 9 runs can predict the EAWM index well in UKMO, but it leaves the failure of the remaining 7 runs unexplained, which is beyond the scope of the current study.

TABLE 3. Correlation coefficients between the observed and the nine-run ensemble EAWM indices in DEMETER CGCMs for the indices proposed in this paper (New index) and in 12 other papers listed in the references. The choice of the 12 indices has two criteria. First, the correlation coefficient between the index and the winter-mean East Asian surface air temperature exceeds −0.50 (Fig. 5). Second, the variables used for the definition of the index are available in the outputs of DEMETER CGCMs. One and two asterisks (* and **) indicate that the correlation coefficients exceed the 99% and 99.9% confidence levels based on a two-sided Student's *t* test, respectively.

	SCWF (ECMWF)	CNRM (Météo-France)	UKMO (UK Met Office)
New index	−0.07	0.52**	0.22
Guo (1994)	0.00	0.31	−0.27
Shi (1996)	0.00	0.36	0.02
Wu and Wang (2002)	−0.04	0.31	−0.11
Chan and Li (2004)	−0.06	0.22	−0.28
Wang et al. (2009b)	−0.04	0.16	−0.19
Chen et al. (2000)	0.61**	0.67**	0.58**
Hu et al. (2000)	0.49**	0.65**	0.50**
Zhu (2008)	−0.09	0.36	0.00
Li and Yang (2010)	0.21	0.39*	0.15
Cui and Sun (1999)	0.09	0.46*	0.29
Sun and Li (1997)	−0.01	0.48*	0.29
Wang et al. (2009a)	0.18	−0.16	−0.21

6. Summary

The thermal contrast (SLP gradient) between the Asian continent and the adjacent oceans is the primary nature of the EAWM. The east–west pressure gradient between the Siberian high and the Aleutian low has been widely used to define the EAWM index, while the north–south pressure contrast between the Siberian high and the MC low was less taken into account in EAWM studies. Therefore, based on SLP data, a new index is proposed to measure the intensity of the EAWM by explicitly taking into account both the east–west and the north–south pressure gradients. The new index can capture both the interannual and the interdecadal variations of the EAWM reported in previous studies well. The represented circulations feature a deepened mid-tropospheric East Asian trough, sharpened and accelerated upper-tropospheric East Asian jet stream, and enhanced lower-tropospheric northerly winds in strong EAWM winters. Accordingly, the surface air temperature is significantly below normal over East Asia, and the precipitation is enhanced (suppressed) over the Maritime Continent (along the EAWM front extending from southeast China to the northwest Pacific). The climate anomalies are opposite in weak EAWM winters. Compared with previous EAWM indices, this new index has a distinct advantage in describing the interannual variations of the EAWM and the related winter-mean surface air temperature over East Asia, especially for the extreme warm and cold cases. A further comparison between the new index and previous EAWM indices can be found in section 7c.

The proposed EAWM index has a close relationship with several atmospheric teleconnections such as AO, EU, and NPO/WP. Compared with the zonally asymmetric AO, the EU and NPO/WP patterns show a closer relationship with the EAWM index. In fact, some recent studies also suggest that the EU-like and WP-like anomalies are very important for the interannual variations of the EAWM (e.g., Li et al. 2007; L. Wang et al. 2010; Liu and Chen 2012; Liu et al. 2014, manuscript submitted to *Climate Dyn.*; Takaya and Nakamura 2013). Hence, this index could be a good choice to study the mechanism of the EAWM especially from the perspective of the EU and NPO/WP patterns. Regarding the associations with the atmospheric external forcing, the new index reveals a close relationship with ENSO and the Arctic sea ice, consistent with previous studies. On the other hand, some previous studies implied associations between the EAWM and SST/atmospheric anomalies over the Indian Ocean (e.g., Chen et al. 2000; Wu et al. 2006). Such a relationship is well depicted with this new index. Moreover, it is suggested that the SST anomalies over the tropical Indian Ocean are more closely related to the EAWM index as an independent potential predictor especially from late autumn to early winter. This may add further knowledge to the prediction potentials of the EAWM apart from ENSO. The analysis of three DEMETER CGCMs suggests that the predictability of this new index is good in CNRM and poor in UKMO and SCWF. This may be related to the ability of the models in reproducing the EAWM variability and the relationship between the EAWM and the tropical oceans.

7. Discussion

a. Relative importance of the east–west and the north–south SLP gradients to the EAWM variability

The inclusion of the north–south pressure gradient is one merit of our EAWM index. One may ask whether it is the east–west or the north–south gradient that plays a more important role in the EAWM variability. To answer this question, first, two indices that only consist of the east–west (north–south) SLP gradient were constructed based on the areas indicated in Fig. 1. The time series of the east–west index (EWI) and the north–south index (NSI) based on raw SLP are shown in Fig. 9. The similar magnitude of the two indices implies the comparable roles of the east–west and the north–south SLP gradients to the EAWM variability. The correlation coefficient between our EAWM index and the EWI (NSI) is 0.95 (0.91) (Table 4), confirming their almost equivalent contribution to the EAWM variability. Second, we examined the climate anomalies associated with EWI and NSI. The circulation anomalies represented by the two indices quite resemble to each other. The main difference between them is that the circulation anomalies associated with the EWI (NSI) are stronger to the north (south) of about 30°N (not shown). Besides, the 850-hPa wind anomalies associated with the EWI (NSI) feature a slightly higher (lower) confidence level. Hence, it suggests that the roles played by the east–west SLP gradient that reflects the midlatitude geostrophic processes seem to be a little more important than those played by the north–south SLP gradient that reflects the local Hadley circulation in the variability of the EAWM, although the two gradients have almost equivalent importance.

On the other hand, the correlation coefficient between NSI and EWI is 0.74 (Table 4), suggesting that they only share about 55% of covariance. The relative independence of the two indices highlights the necessity of considering both the north–south and the east–west SLP gradients in the EAWM index. A closer inspection reveals that the relationship between the Siberian high and the MC low is slightly tighter than that between the

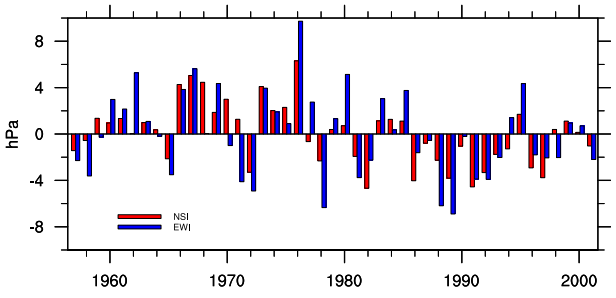

FIG. 9. DJF-mean EWI and NSI based on raw SLP for the period 1957–2001.

TABLE 4. Correlation coefficients among the DJF-mean Siberian high index (SH), the Aleutian low index (AL), the Maritime low index (MC), the north–south pressure gradient index (NSI), the east–west pressure gradient index (EWI), and the EAWM index (EAWMI) based on raw SLP (value to the left of the slash) and normalized SLP (value to the right of the slash) for the period 1957–2001.

	SH	AL	MC	NSI	EWI
EAWMI	0.91/0.89	0.64/0.58	0.48/0.61	0.91/0.92	0.95/0.91
EWI	0.78/0.81	0.83/0.81	0.29/0.30	0.74/0.67	—
NSI	0.94/0.82	0.29/0.26	0.66/0.82	—	—
MC	0.35/0.35	0.12/0.12	—	—	—
AL	0.30/0.30	—	—	—	—

Siberian high and the Aleutian low (Table 4). This is probably due to the intense tropical–extratropical interactions associated with cold surges of the EAWM (Chang et al. 2006, 2011), which has a clear and straightforward physical meaning. The inclusion of this physically meaningful north–south SLP gradient may be an important reason for the improved performance of our EAWM index.

Here, we briefly revisit how the Maritime Continent influences the EAWM due to its contribution to the north–south SLP gradient. On one hand, the enhanced Maritime Continent convection is often associated with a La Niña–like SST pattern on the interannual time scale. This SST pattern excites cyclonic anomalies and significant northerly wind anomalies in the lower troposphere over the western North Pacific, facilitating a strong EAWM (Wang et al. 2000). On the other hand, a recent study suggests that the variations of the Maritime Continent convection could excite an upper-tropospheric Rossby wave train emanating from the tropics to the midlatitude East Asia (Zheng et al. 2013). This wave train could modulate the strength of the East Asian trough and in turn lead to changes of the EAWM strength.

b. *Choice of raw and normalized SLP*

In this study, the EAWM index is defined with the normalized area-averaged SLP instead of the raw SLP. This procedure naturally increases the weighting of the tropics due to the relatively small interannual variance of the tropical SLP (Fig. 1b). A closer inspection reveals that it increases the weighting of the MC low and decreases the weighting of the Aleutian low, with the weighting of the Siberian high being almost unchanged (Table 4). However, this normalization procedure does not lead to obvious difference between our index and that based on the raw SLP except better performance of our index in DEMETER CGCMs. The time series of our index is almost identical to that using the raw SLP (not shown). The correlation coefficient between the two indices is 0.99 for the 45 years concerned. The climate anomalies associated with the two indices (i.e., the analyses in Figs. 3–7) are almost indistinguishable (not shown). In contrast, the correlation coefficient between the observed and predicted indices in CNRM model falls from 0.52 to 0.44 when the normalized SLP is replaced by the raw SLP. This is understandable because usually the tropics are a main source of predictability in most of the CGCMs. The normalization procedure reinforces the role of the tropics and in turn increases the predictability of the index in models. Hence, it is optimal to use the normalized SLP in our index.

c. *A further comparison with previous EAWM indices*

The formation and variability of the EAWM is related to both the tropical and the extratropical factors, while previous indices usually well reflect only one aspect of this relationship (Wang and Chen 2010). For example, the indices based on low-level meridional wind are closely associated with the tropical SST but not so closely related to the midlatitude teleconnections. In contrast, the new index is closely linked to both the tropical and the extratropical factors (e.g., Figs. 3 and 7 and Table 2), possibly due to the combination of both the east–west and the north–south SLP gradients and the resultant better representation of the nature of the EAWM. This obvious improvement in turn leads to a better performance of the new index in describing the wintertime surface air temperature anomalies associated with the EAWM (Figs. 4–6), even in the area with complex topography (i.e., the area right to the east of the Tibetan Plateau) where most of the previous indices failed (Wang and Chen 2010).

Predictability in CGCMs is an important criterion for the index. In this aspect, the indices based on low-level meridional wind have an overwhelming advantage (Table 3). The indices defined by Chen et al. (2000) and Hu et al. (2000) have significant predictability in all the three CGCMs concerned. This is possible because

the two indices have a very close relationship with ENSO (Wang and Chen 2010) and ENSO is a main source of predictability in CGCMs (e.g., Jiang et al. 2013). In contrast, the new index only has high predictability in CNRM model, but it ranks number 3 among all the indices in Table 3. Given the relatively lower performance of the Chen et al. (2000) and Hu et al. (2000) indices in describing the East Asian temperature (Figs. 5h,i and 6h,i), the new index could be a good choice for the monitoring and prediction of the EAWM in operational climate centers. Last but not the least, SLP data are available for a very long period with good data quality compared with other atmospheric variables. Some widely used SLP data can be traced back to the year 1850. Hence, the new index is a reliable and suitable choice to investigate the historical variations of the EAWM in addition to the EAWM variations in recent decades.

Acknowledgments. We thank the three anonymous reviewers for their insightful comments and suggestions. This work was supported by the National Natural Science Foundation of China (41230527, 41025017), the National Department Public Benefit Research Foundation of China (GYHY201406039), and the Chinese Academy of Sciences (KZCX2-EW-QN204).

REFERENCES

Alory, G., S. Wijffels, and G. Meyers, 2007: Observed temperature trends in the Indian Ocean over 1960–1999 and associated mechanisms. *Geophys. Res. Lett.,* **34,** L02606, doi:10.1029/2006GL028044.

Annamalai, H., P. Liu, and S. P. Xie, 2005: Southwest Indian Ocean SST variability: Its local effect and remote influence on Asian monsoons. *J. Climate,* **18,** 4150–4167.

Boo, K. O., G. Martin, A. Sellar, C. Senior, and Y. H. Byun, 2011: Evaluating the East Asian monsoon simulation in climate models. *J. Geophys. Res.,* **116,** D01109, doi:10.1029/2010JD014737.

Chan, J. C. L., and C. Y. Li, 2004: The East Asia winter monsoon. *East Asian Monsoon,* C. P. Chang, Ed., World Scientific, 54–106.

Chang, C.-P., Z. Wang, and H. Hendon, 2006: The Asian winter monsoon. *The Asian Monsoon,* B. Wang, Ed., Springer, 89–127.

——, M.-M. Lu, and B. Wang, 2011: The East Asian winter monsoon. *The Global Monsoon System: Research and Forecast,* C.-P. Chang et al., Eds., World Scientific Series on Asia-Pacific Weather and Climate, Vol. 5, World Scientific, 99–109.

Chen, J., and S. Q. Sun, 1999: East Asian winter monsoon anomaly and variation of global circulation. Part I: A comparison study on strong and weak winter monsoon. *Chin. J. Atmos. Sci.,* **23,** 101–111.

Chen, M., P. Xie, J. Janowiak, and P. Arkin, 2002: Global land precipitation: A 50-yr monthly analysis based on gauge observations. *J. Hydrometeor.,* **3,** 249–266.

——, ——, ——, ——, and T. Smith, 2003: Reconstruction of the oceanic precipitation from 1948 to the present. *Extended Abstracts, 14th Symp. on Global Changes and Climate Variations,* Long Beach, CA, Amer. Meteor. Soc., 3.5. [Available online at https://ams.confex.com/ams/annual2003/techprogram/paper_54461.htm.]

Chen, W., H. F. Graf, and R. H. Huang, 2000: The interannual variability of East Asian winter monsoon and its relation to the summer monsoon. *Adv. Atmos. Sci.,* **17,** 48–60.

Cui, X. P., and Z. B. Sun, 1999: East Asian winter monsoon index and its variation analysis. *J. Nanjing Inst. Meteor.,* **22,** 321–325.

Gong, D. Y., S. W. Wang, and J. H. Zhu, 2001: East Asian winter monsoon and Arctic Oscillation. *Geophys. Res. Lett.,* **28,** 2073–2076.

Guo, Q. Y., 1994: Relationship between the variations of East Asian winter monsoon and temperature anomalies in China (in Chinese). *Quart. J. Appl. Meteor.,* **5,** 218–225.

Honda, M., J. Inoue, and S. Yamane, 2009: Influence of low Arctic sea-ice minima on anomalously cold Eurasian winters. *Geophys. Res. Lett.,* **36,** L08707, doi:10.1029/2008GL037079.

Hu, Z.-Z., L. Bengtsson, and K. Arpe, 2000: Impact of global warming on the Asian winter monsoon in a coupled GCM. *J. Geophys. Res.,* **105** (D4), 4607–4624.

Jhun, J. G., and E. J. Lee, 2004: A new East Asian winter monsoon index and associated characteristics of the winter monsoon. *J. Climate,* **17,** 711–726.

Ji, L. R., S. Q. Sun, K. Arpe, and L. Bengtsson, 1997: Model study on the interannual variability of Asian winter monsoon and its influence. *Adv. Atmos. Sci.,* **14,** 1–22.

Jiang, X., S. Yang, Y. Li, A. Kumar, W. Wang, and Z. Gao, 2013: Dynamical prediction of the East Asian winter monsoon by the NCEP Climate Forecast System. *J. Geophys. Res. Atmos.,* **118,** 1312–1328, doi:10.1002/jgrd.50193.

Lau, K.-M., C.-P. Chang, and P. H. Chan, 1983: Short-term planetary-scale interactions over the tropics and midlatitudes. Part II: Winter-MONEX period. *Mon. Wea. Rev.,* **111,** 1372–1388.

Lau, N.-C., and M. J. Nath, 1996: The role of the ''atmospheric bridge'' in linking tropical Pacific ENSO events to extratropical SST anomalies. *J. Climate,* **9,** 2036–2057.

Li, F., and H. Wang, 2012: Predictability of the East Asian winter monsoon interannual variability as indicated by the DEMETER CGCMS. *Adv. Atmos. Sci.,* **29,** 441–454.

Li, Y., and S. Yang, 2010: A dynamical index for the East Asian winter monsoon. *J. Climate,* **23,** 4255–4262.

——, R. Lu, and J. H. He, 2007: Several climate factors influencing the winter temperature over China. *Chin. J. Atmos. Sci,* **31,** 505–514.

Linkin, M. E., and S. Nigam, 2008: The North Pacific Oscillation–west Pacific teleconnection pattern: Mature-phase structure and winter impacts. *J. Climate,* **21,** 1979–1997.

Liu, S., 2007: A method for determining intensity index of East Asian winter monsoon. *Sci. Geogr. Sin.,* **27,** 10–18.

Liu, Y. Y., and W. Chen, 2012: Variability of the Eurasian teleconnection pattern in the Northern Hemisphere winter and its influences on the climate in China. *Chin. J. Atmos. Sci,* **36,** 423–432.

Lu, E., and J. C. L. Chan, 1999: A unified monsoon index for south China. *J. Climate,* **12,** 2375–2385.

Nakamura, H., T. Izumi, and T. Sampe, 2002: Interannual and decadal modulations recently observed in the Pacific storm track activity and East Asian winter monsoon. *J. Climate,* **15,** 1855–1874.

Neale, R., and J. Slingo, 2003: The Maritime Continent and its role in the global climate: A GCM study. *J. Climate,* **16,** 834–848.

Palmer, T. N., and Coauthors, 2004: Development of a European Multimodel Ensemble System for Seasonal-To-Interannual Prediction (DEMETER). *Bull. Amer. Meteor. Soc.,* **85,** 853–872.

Rayner, N. A., D. E. Parker, E. B. Horton, C. K. Folland, L. V. Alexander, D. P. Rowell, E. C. Kent, and A. Kaplan, 2003: Global analyses of sea surface temperature, sea ice, and night marine air temperature since the late nineteenth century. *J. Geophys. Res.,* **108,** 4407, doi:10.1029/2002JD002670.

Shi, N., 1996: Features of the East Asian winter monsoon intensity on multiple time scale in recent 40 years and their relation to climate (in Chinese). *Quart. J. Appl. Meteor.,* **7,** 175–182.

Sun, B. M., and C. Y. Li, 1997: Relationship between the disturbances of East Asian trough and tropical convective activities in boreal winter. *Chin. Sci. Bull.,* **42,** 500–504.

Takaya, K., and H. Nakamura, 2005: Mechanisms of intraseasonal amplification of the cold Siberian high. *J. Atmos. Sci.,* **62,** 4423–4440.

——, and ——, 2013: Interannual variability of the East Asian winter monsoon and related modulations of the planetary waves. *J. Climate,* **26,** 9445–9461.

Thompson, D. W. J., and J. M. Wallace, 1998: The Arctic Oscillation signature in the wintertime geopotential height and temperature fields. *Geophys. Res. Lett.,* **25,** 1297–1300.

Trenberth, K. E., G. W. Branstator, D. Karoly, A. Kumar, N. C. Lau, and C. Ropelewski, 1998: Progress during TOGA in understanding and modeling global teleconnections associated with tropical sea surface temperatures. *J. Geophys. Res.,* **103** (C7), 14 291–14 324.

——, J. Hurrell, and D. Stepaniak, 2006: The Asian monsoon: Global perspectives. *The Asian Monsoon,* B. Wang, Ed., Springer, 67–87.

Uppala, S. M., and Coauthors, 2005: The ERA-40 Re-Analysis. *Quart. J. Roy. Meteor. Soc.,* **131,** 2961–3012.

Wallace, J. M., and D. S. Gutzler, 1981: Teleconnections in the geopotential height field during the Northern Hemisphere winter. *Mon. Wea. Rev.,* **109,** 784–812.

Wang, B., R. Wu, and X. Fu, 2000: Pacific–East Asian teleconnection: How does ENSO affect East Asian climate? *J. Climate,* **13,** 1517–1536.

——, Z. Wu, C.-P. Chang, J. Liu, J. Li, and T. Zhou, 2010: Another look at interannual-to-interdecadal variations of the East Asian winter monsoon: The northern and southern temperature modes. *J. Climate,* **23,** 1495–1512.

Wang, H. J., and D. B. Jiang, 2004: A new East Asian winter monsoon intensity index and atmospheric circulation comparison between strong and weak composite. *Quat. Sci.,* **24,** 19–27.

Wang, L., and W. Chen, 2010: How well do existing indices measure the strength of the East Asian winter monsoon? *Adv. Atmos. Sci.,* **27,** 855–870, doi:10.1007/s00376-009-9094-3.

——, and J. Feng, 2011: Two major modes of the wintertime precipitation over China. *Chin. J. Atmos. Sci.,* **35,** 1105–1116.

——, and W. Chen, 2014: The East Asian winter monsoon: Reamplification in the mid-2000s. *Chin. Sci. Bull.,* **59,** 430–436, doi:10.1007/s11434-013-0029-0.

——, ——, W. Zhou, and R. Huang, 2009a: Interannual variations of East Asian trough axis at 500 hPa and its association with the East Asian winter monsoon pathway. *J. Climate,* **22,** 600–614.

——, R. Huang, L. Gu, W. Chen, and L. Kang, 2009b: Interdecadal variations of the East Asian winter monsoon and their association with quasi-stationary planetary wave activity. *J. Climate,* **22,** 4860–4872.

——, W. Chen, W. Zhou, J. C. L. Chan, D. Barriopedro, and R. H. Huang, 2010: Effect of the climate shift around mid-1970s on the relationship between wintertime Ural blocking circulation and East Asian climate. *Int. J. Climatol.,* **30,** 153–158.

Watanabe, M., and F.-F. Jin, 2002: Role of Indian Ocean warming in the development of Philippine Sea anticyclone during ENSO. *Geophys. Res. Lett.,* **29,** 1478, doi:10.1029/2001GL014318.

Wu, B., and J. Wang, 2002: Winter Arctic Oscillation, Siberian high and East Asian winter monsoon. *Geophys. Res. Lett.,* **29,** 1897, doi:10.1029/2002GL015373.

——, R. Huang, and D. Gao, 1999: Impact of variations of winter sea-ice extents in the Kara/Barents Seas on winter monsoon over East Asia. *Acta Meteor. Sin.,* **13,** 141–153.

——, R. Zhang, and R. D'Arrigo, 2006: Distinct modes of the East Asian winter monsoon. *Mon. Wea. Rev.,* **134,** 2165–2179.

——, J. Su, and R. Zhang, 2011: Effects of autumn–winter Arctic sea ice on winter Siberian high. *Chin. Sci. Bull.,* **56,** 3220–3228.

Xu, S. Y., and J. J. Ji, 1965: The climate and weather features during the outbreak period of China's winter monsoon. *Geogr. Symp.,* **9,** 85–101.

Yang, S., K. M. Lau, and K. M. Kim, 2002: Variations of the East Asian jet stream and Asian–Pacific–American winter climate anomalies. *J. Climate,* **15,** 306–325.

Zhang, Y., K. R. Sperber, and J. S. Boyle, 1997: Climatology and interannual variation of the East Asian winter monsoon: Results from the 1979–95 NCEP/NCAR reanalysis. *Mon. Wea. Rev.,* **125,** 2605–2619.

Zheng, J., Q. Liu, C. Wang, and X.-T. Zheng, 2013: Impact of heating anomalies associated with rainfall variations over the Indo-western Pacific on Asian atmospheric circulation in winter. *Climate Dyn.,* **40,** 2023–2033.

Zhu, Y. F., 2008: An index of East Asian winter monsoon applied to the description of China's mainland winter temperature changes. *Acta Meteor. Sin.,* **22,** 522–529.